



McGhee, J., Moran, D. A. and Georgiev, V. P. (2019) Simulations of Surface Transfer Doping of Hydrogenated Diamond by MoO<sub>3</sub> Metal Oxide. In: 2019 Joint International EUROSIOI Workshop and International Conference on Ultimate Integration on Silicon (EUROSIOI-ULIS), Grenoble, France, 01-03 Apr 2019, ISBN 9781728116587.

There may be differences between this version and the published version. You are advised to consult the publisher's version if you wish to cite from it.

<http://eprints.gla.ac.uk/214872/>

Deposited on: 27 April 2020

Enlighten – Research publications by members of the University of Glasgow  
<http://eprints.gla.ac.uk>

# Simulations of Surface Transfer Doping of Hydrogenated Diamond by MoO<sub>3</sub> metal oxide

Joseph McGhee<sup>1,2</sup>, David A. Moran<sup>2</sup>, Vihar P. Georgiev<sup>1</sup>

<sup>1</sup>Device Modeling Group, University of Glasgow, Glasgow G128LT, Scotland, UK

<sup>2</sup>Nano Electronic Diamond Devices and Systems Group, University of Glasgow, Glasgow G128LT, Scotland, UK  
[vihar.georgiev@glasgow.ac.uk](mailto:vihar.georgiev@glasgow.ac.uk)

**Abstract**—In this work we investigate the surface transfer doping effect induced between hydrogen terminated diamond and MoO<sub>3</sub>. We simulated the interface of (100) MoO<sub>3</sub> surface and hydrogen terminated (100) diamond surface using first principle methods such as Density Functional Theory (DFT). DFT simulation allowed us to calculate the band structure and charge transfer between the MoO<sub>3</sub> and the diamond materials. Analysis of the band structures and density of states shows that the MoO<sub>3</sub> is an electron acceptor and injects holes into the diamond structure.

**Keywords**—Surface transfer doping (STD); 2D hole gas (2DHG), diamond

## I. INTRODUCTION

Diamond has unique properties that make it an attractive wide band-gap material to produce future high-performance electronic devices. With a wide band-gap of 5.5eV, a thermal conductivity 5 times greater than 4H-SiC of 24 W/cm<sup>2</sup>K (for CVD diamond), a high breakdown field of 20Wcm<sup>-1</sup> and high hole and electron carrier velocities of 0.8x10<sup>7</sup>cm/s and 2.0x10<sup>7</sup>cm/s respectfully, diamond is a clear stand out candidate for high frequency and high power devices [1-3]. However, the lack of a suitable doping mechanism has hindered the application of diamond in electronic devices. Conventional substitutional doping is not an ideal option as it is difficult to substitute atoms into the diamond crystal lattice, limiting the potential for diamond to be used as a semiconductor in electronic applications [4]. It is possible to dope diamond with some atoms, boron being the most common. Boron doping has its limitations however - as the doping concentration is increased the hole mobility deteriorates and at doping concentrations above 3.9x10<sup>21</sup>cm<sup>-3</sup> the diamond has semi metallic properties; at cryogenic temperatures it becomes superconducting [5]. Surface Transfer Doping (STD) gives the use of diamond for such applications more promise [6]. For STD to occur there are two prerequisites: hydrogen terminated diamond (H-diamond) and an electron accepting material in intimate contact with the H-diamond. The hydrogen termination gives the diamond a negative electron affinity which facilitates the transfer

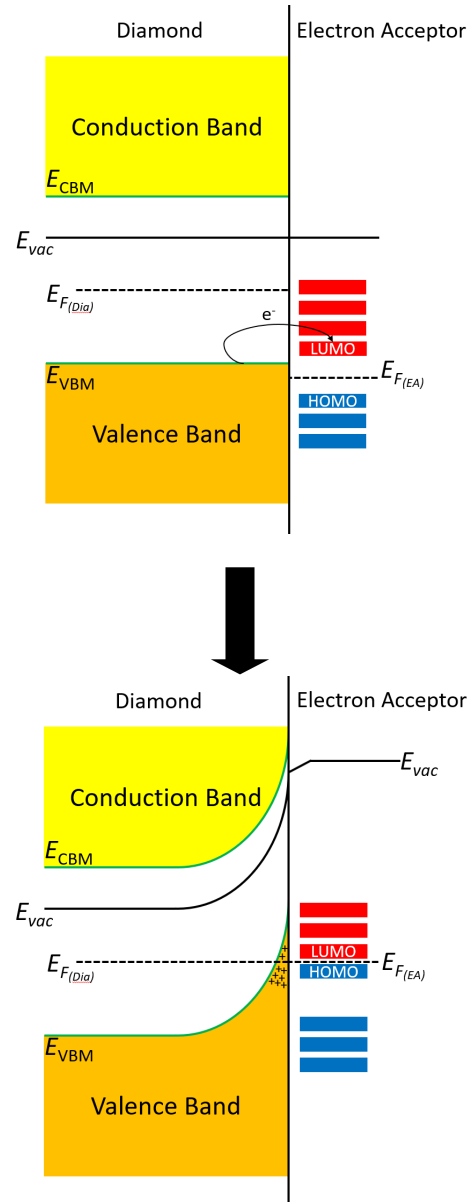


Figure 1. Band diagrams showing the interaction of hydrogen terminated diamond with a surface acceptor material.

of electrons from the diamond to the accepting material, creating a quasi two-dimensional hole gas (2DHG) in the diamond.

Figure 1 shows the band bending mechanism in the

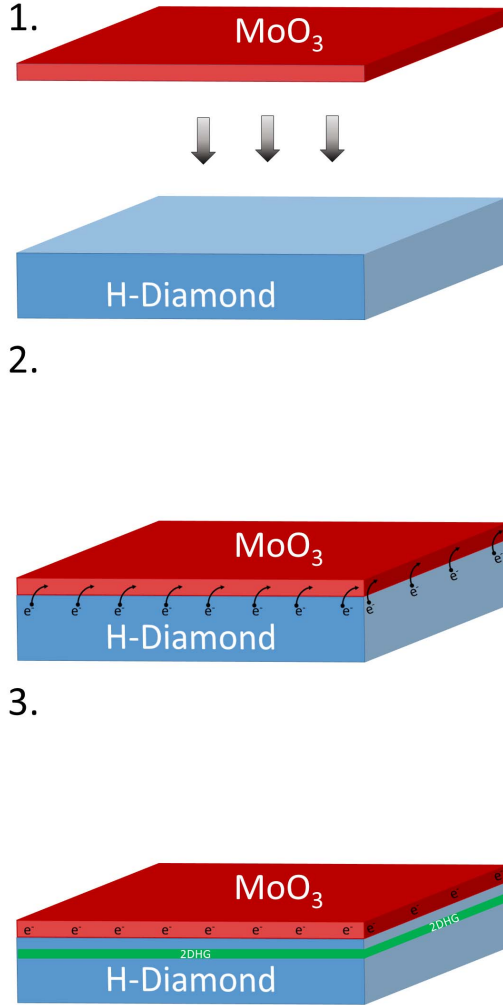


Figure 2. The creation of the 2DHG just below the diamond surface after interfaced with  $\text{MoO}_3$ .

H-diamond when it comes in contact with an electron acceptor. In the earliest developments of STD the accepting material was provided by molecules in the atmosphere spontaneously adsorbed onto the surface of hydrogen terminated diamond. However, the lack of control over the adsorption of these atmospheric molecules, and the fact they are readily desorbed by fabrication processes and raised temperatures, has led to research into alternative electron acceptors that can be controlled, are more stable and improve reliability [6].

One of the materials that has been experimentally proven to improve the performance and stability of

STD is  $\text{MoO}_3$  [7]. Figure 2 represents a schematic diagram which shows that when  $\text{MoO}_3$  is deposited on H-diamond electrons from just below the surface of the diamond ( $\sim 10\text{nm}$ ) will transfer to the  $\text{MoO}_3$  creating the 2DHG.

In order to investigate this hypothesis and mechanism in more detail, in this work we present Density Functional Theory (DFT) simulations investigating the processes of STD in diamonds. The theoretical study of the interface between the diamond and different oxides would help give a better understanding of the mechanisms at play and further develop knowledge in the field. Interfaces of (100)  $\alpha\text{-MoO}_3$  and  $2\times 1\text{-(100)}$  H-diamond have been modelled and STD analysed. Establishing a high-performance STD process in the diamond will catalyse research in a wide area of diamond-based applications.

## II. SIMULATION METHODOLOGY

All calculations were carried out with Quantumwise Atomistix ToolKit (ATK) software using DFT[8]. Generalised Gradient Approximation (GGA) exchange correlation was used for the geometry optimisations of all systems and GGA-1/2 exchange correlation was used for all electronic structure calculations. DFT method is well known for underestimating the bandgap of semiconductors [9], therefore to obtain a more accurate electronic description of the systems DFT-1/2 method was used. DFT-1/2 method is a semi-empirical approach which can overcome the error that local and semi-local exchange correlation density functionals inherently have when working with semiconductors and insulators. It works by correcting the self-interaction error of DFT by cancelling out the electron-hole self-interaction energy by defining an atomic self-energy potential [10]. However, DFT-1/2 method is not suitable for calculating properties that depend on total energy, hence, we used GGA for the geometry optimisations. Perdew, Burke and Ernzerhof (PBE) predefined functional was chosen for all calculations. A Monkhorst-Pack scheme with an  $8 \times 8 \times 1$  k-point density ( $\text{\AA}$ ) mesh was used for the Brillouin zone integration.

The H-diamond and  $\text{MoO}_3$  were created and geometry optimised individually. The (100)  $\text{MoO}_3$  was then interfaced with  $2\times 1\text{-(100)}$  H-diamond with a strain of  $<1\%$  being placed on the  $\text{MoO}_3$ . To optimise the interface separation the H-diamond was fixed and the  $\text{MoO}_3$  atoms were rigid for the geometry optimisation calculation. The interface distance was corrected for counterpoise basis set superposition error and van der Waals interactions.

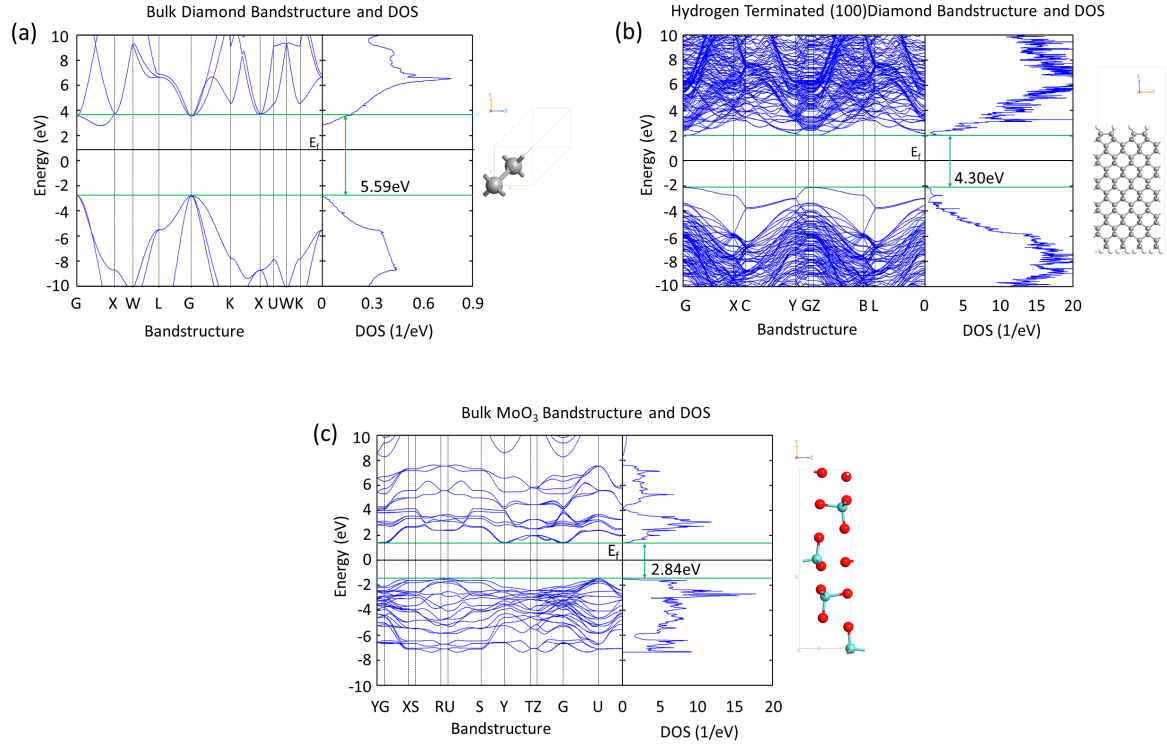


Figure 3. (a) bandstructure and DOS of bulk diamond showing a band gap of 5.59eV, (b) bandstructure and DOS of hydrogen terminated (100) diamond showing a reduced band gap of 4.30eV, (c) bandstructure and DOS of bulk MoO<sub>3</sub> showing a band gap of 2.84eV.

### III. RESULTS AND DISCUSSION

Fig. 3 compares diamond, hydrogen terminated diamond and MoO<sub>3</sub> band structure and DOS obtained from the super cell DFT simulations. The data presented in Fig 3 (a) and (b) shows that when diamond is hydrogen terminated the band gap is slightly reduced at the surface due to surface gap states at the valance band maximum (VBM) because of the presence of hydrogen atoms. Although the band gap has been reduced to 4.30eV when the DOS is projected for carbon atoms in the bulk of the structure the band gap remains ~5.5eV.

The band gap of 2.84eV obtained for MoO<sub>3</sub> (Fig 3(c)) is comparable to reported experimental values between 2.9-3.15eV [11]. MoO<sub>3</sub> is an amorphous material and therefore does not have a well-defined crystal structure. In our simulations the MoO<sub>3</sub> is built as a perfect crystal and this is the reason that the band gap obtained from the DFT is slightly lower than the reported experimental results.

Figure 4 shows the Projected Density of States (PDOS) for the 's' electron shells of the hydrogen and the 'p' electron shells of the carbon atoms before and after the H-diamond has been interfaced with MoO<sub>3</sub>. The PDOS diagram reveals that when the H-diamond

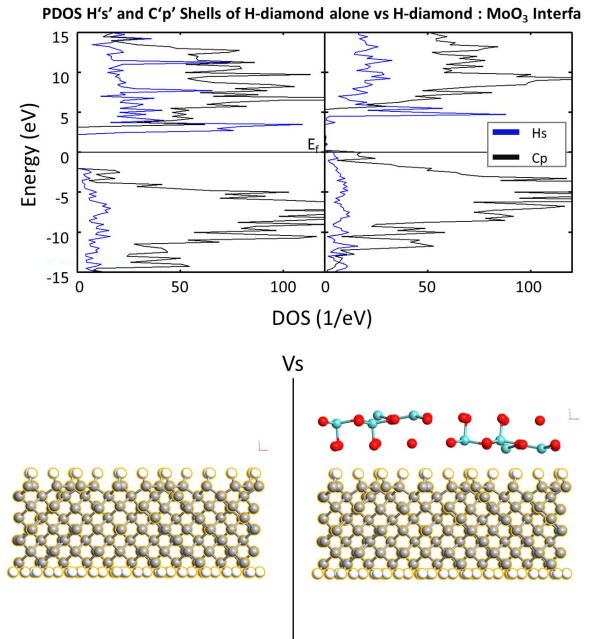


Figure 4. PDOS plots of Hs and Cs shells before and after the H-diamond is interfaced with the oxide. The lower image shows the repeating units of the systems with the atoms highlighted that are being projected in the PDOS plot.

is in contact with the metal oxide there is a shift of the PDOS to higher energies and the Fermi Level ( $E_F$ ) is in contact with the valence states. The band gap of the diamond remains constant but the VBM has moved closer to the  $E_F$  as it crosses the fermi level, which in turn means the conduction band minimum (CBM) also moves upwards, indicating that there has been charge transfer at the interface.

The PDOS plot of the  $H_s$ ,  $C_p$  and  $Mo_d$  shells in Figure 5 shows that the  $Mo_d$  has states that lie within the bandgap of the diamond and can accept electrons. Hence, this result suggests electrons transfer from the diamond to the oxide creating 2DHG in the diamond surface which is in direct contact with the metal oxide.

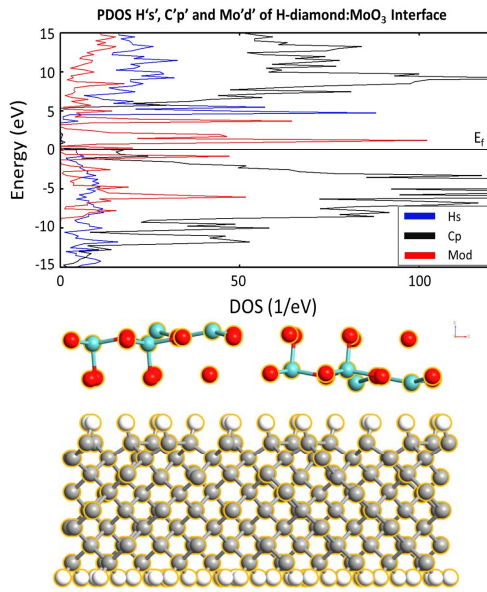


Figure 5. PDOS plot of  $H_s$ ,  $C_s$ , and  $Mod$  shells when the interface is created with the image of the repeating unit of the system below.

Analysis of the Mulliken electron population of the system showed that there was a transfer of 3.6 electrons from the H-diamond to the oxide. Given that the surface area of the system was  $\sim 60\text{\AA} \times 10\text{\AA}$  this would mean that calculating the charge transfer per  $\text{cm}^2$  would be  $\sim 6 \times 10^{13} \text{cm}^{-2}$ . This is comparable to reported experimental values obtained by hall measurements of  $\text{MoO}_3$  deposited on the surface of H-diamond substrates of  $\sim 2.5 \times 10^{13} - 6 \times 10^{13} \text{cm}^{-2}$  carrier concentration [12].

Element	Mulliken Electron Population	
	Isolated element	Average per Atom After Interfaced
C	4	3.5804
H	1	1.3732
Mo	12	12.0097
O	6	6.7141

Table 1. Showing the change in electron population per atom.

Table 1 shows that the average electron population of the carbon atoms in the interfaced system decreased but, the average electron population of the hydrogen, molybdenum and oxygen atoms increased which is due to the charge transfer from the diamond through the hydrogen atoms to the  $\text{MoO}_3$ . It also suggests that the majority of the charge transfer goes to the oxygen.

#### IV. CONCLUSION

In this work we investigated the surface transfer doping effect induced between hydrogen terminated diamond and  $\text{MoO}_3$ . We simulated the interfaces of (100)  $\text{MoO}_3$  and hydrogen terminated (100) diamond using DFT calculations. The PDOS data shows there is shift of the VBM and CBM bands of the H-diamond and there is charge transfer between the diamond and the metal oxide. The oxide readily acts as an electron acceptor to the diamond and creates a 2DHG in the diamond. The carrier concentration in the diamond has been calculated to be  $6 \times 10^{13} \text{cm}^{-2}$  which is similar to experimental values of single crystal H-diamond substrates with a deposited layer of  $\text{MoO}_3$ .

#### REFERENCES

1. Wort, C. and R. Balmer, *Diamond as an Electronic material*. Materials Today, 2008. **11**(1).
2. Russell, S., et al., *RF Operation of Hydrogen-Terminated Diamond Field Effect Transistors*. IEEE, 2015. **62**(3).
3. Kitabayashi, Y., et al., *Normally-Off C-H Diamond MOSFETs With Partial C-O Channel Achieving 2-kV Breakdown Voltage*. IEEE Electron Device Letters, 2017. **38**(3): p. 363-366.
4. Zhou, D., et al., *Synthesis and electron field emission of nanocrystalline diamond thin films grown from  $N_2/CH_4$  microwave plasmas*. Journal of Applied Physics, 1997. **82**(9): p. 4546-4550.
5. Yokoya, T., et al., *Origin of the metallic properties of heavily boron-doped superconducting diamond*. Nature, 2005. **438**: p. 647.
6. Crawford, K., et al., *Enhanced surface transfer doping of diamond by  $V_2O_5$  with improved thermal stability*. Applied Physics Letters, 2016. **108**(4).
7. Russell, S., et al., *Surface transfer doping of diamond by  $MoO_3$ : a combined spectroscopic and Hall measurement study*. Applied Physics Letters, 2013. **103**(20).
8. (2017.2), A.T., *Atomistix ToolKit (2017.2)*. Atomistix ToolKit (2017.2) QuantumWise A/S.
9. Edmonds, M., et al., *Spin-Orbit Interaction in a Two-Dimensional Hole Gas at the Surface of Hydrogenated Diamond*. Nano Letters, 2015. **15**(1): p. 16-20.
10. Ferreira, L.G., M. Marques, and L.K. Teles, *Slater half-occupation technique revisited: the LDA-1/2 and GGA-1/2 approaches for atomic ionization energies and band gaps in semiconductors*. AIP Advances, 2011. **1**(3): p. 032119.
11. K. C. S., et al., *Electronic properties of  $MoS_2/MoO_x$  interfaces: Implications in Tunnel Field Effect Transistors and Hole Contacts*. Scientific Reports, 2016. **6**: p. 33562.
12. Crawford, K.G., et al., *Thermally Stable, High Performance Transfer Doping of Diamond using Transition Metal Oxides*. Scientific Reports, 2018. **8**(1): p. 3342.